Chinese Chemical Letters 33 (2022) 4335–4338

Contents lists available at ScienceDirect

Chinese Chemical Letters

journal homepage: www.elsevier.com/locate/cclet

Kinetic characterization of a slow chemical exchange between two sites in *N,N*-dimethylacetylamide by CEST NMR spectroscopy

Lixia Wang[a], Jikun Li[a], Junfeng Xiang[a,b,*], Jie Cui[a], Yalin Tang[a,b,*]

[a] *Beijing National Laboratory for Molecular Sciences (BNLMS), Center for Molecular Sciences, Institute of Chemistry, Chinese Academy of Sciences, Beijing 100190, China*

[b] *University of Chinese Academy of Sciences, Beijing 100049, China*

ARTICLE INFO

Article history:
Received 5 October 2021
Revised 9 January 2022
Accepted 9 January 2022
Available online 15 January 2022

Keywords:
Chemical exchange saturation transfer (CEST)
Chemical exchange
N,N-Dimethylacetylamid
Bloch-McConnell equation
Dynamic kinetics

ABSTRACT

Nuclear magnetic resonance (NMR) spectroscopy has provided many powerful tools for the study of dynamic processes. Among the reported methods, chemical exchange saturation transfer (CEST) is more suitable for systems with slow exchange rates, and there will be promising in the detection and dynamic mechanism of metastable substances. It has been widely used in magnetic resonance imaging (MRI), however whether it is applicable in the field of chemical kinetics needs more examples. Here we studied, as a proof of concept, the kinetics of the slow chemical exchange between the two *N*-methyl protons of *N,N*-dimethylacetylamide (DMA), exploiting QUantifying Exchange using Z-spectrum (QUEZS) and QUantifying Exchange using Saturation Time (QUEST) methods. It turned out that both of QUEZS and QUEST could give the corresponding exchange rates, showcasing the capability of this method to provide accurate kinetic data under a range of temperatures. Our results clearly demonstrated the reliability of CEST-based techniques as a tool for dynamic kinetics by NMR.

Nuclear magnetic resonance (NMR) spectroscopy is a key method to reveal the information about atomic arrangements, and further uncover the fine structures of unknown compounds. In addition, NMR technologies, with their high spatial resolution, can not only give chemical shifts and coupling constants, but also provide chemical intuition for the interactions between atoms, such as electrostatic interaction [1,2], hydrogen bond binding [3–6], van der Waals force interaction [7], CH•••π stacking [8,9]. During an NMR experiment, many different physical processes cause relaxation, such as molecular vibration, molecular rotation, chemical exchange, and macroscopic diffusion [10]. For slow exchange where the line widths of NMR signals are almost unaffected by the dynamic processes, the observation of signal coalescence is very restricted or even impossible. A total line shape analysis often proved to be inapplicable [11].

Chemical exchange saturation transfer (CEST) is based on the original saturation transfer experiments by Forsen and Hoffman [12] and is widely used to encode chemical information in magnetic resonance imaging (MRI) [13–15]. Its basic principle is to use selective radio frequency pulses to saturate exchangeable protons and transfer saturated protons to free water through chemical exchange, resulting in a decrease in the signal of the water pool. CEST NMR could thereby help the researchers infer information on the solute pool and the environment around it. Plotting the normalized longitudinal magnetization against the applied saturation frequency, we could obtain the CEST Z-spectrum. It does not require any pre-knowledge of chemical shifts, and could detect invisible substances, owing to its high sensitivity. For example, it can be used to detect active substances in living organisms [16,17], study the kinetics of organic reactions [18,19] and the dynamics of conformational transitions [20–22]. Compared with other chemical exchange measurement techniques, such as exchange spectroscopy (EXSY), Carr-Purcell-Meiboom-Gill (CPMG), spin-relaxation in the rotating frame ($R_{1\rho}$), CEST is more suitable for systems with slow exchange rates [23]. As far as we know, CEST experiment is more sensitive to proton exchange, and the measurable exchange rate constant is in the range of 50,000~1 s^{-1} [24]. More and more experiments show that CEST NMR could enhance sensitivity more than 10-fold [25,26], More importantly, it does not alter the reaction system as it does not require external reagents, such as radicals and para hydrogen [18]. The CEST Z-spectrum can intuitively reflect the kinetic information of the exchange process between two sites. And the rate constants coming from CEST Z-spectrum

* Corresponding authors at: Beijing National Laboratory for Molecular Sciences (BNLMS), Center for Molecular Sciences, Institute of Chemistry, Chinese Academy of Sciences, Beijing 100190, China

E-mail addresses: jfxiang@iccas.ac.cn (J. Xiang), tangyl@iccas.ac.cn (Y. Tang).

https://doi.org/10.1016/j.cclet.2022.01.022
1001-8417/

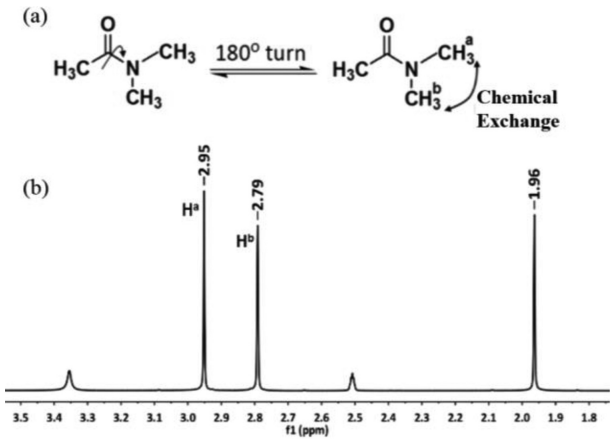

Fig. 1. (a) The scheme for the chemical exchange between protons H^a and H^b in DMA; (b) its ^1H NMR spectrum in DMSO–d_6 at 298 K.

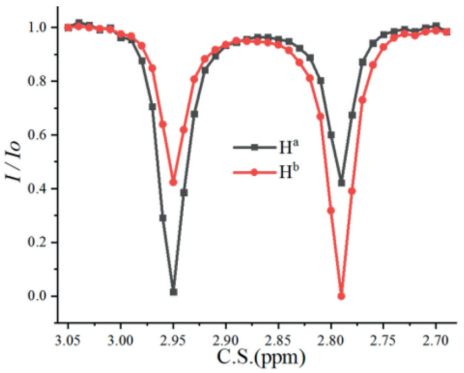

Fig. 2. CEST Z-Spectrum of H^a and H^b at 298 K.

are calculated by fitting the data to the classic Bloch-McConnell equations [27–29]. Its accuracy, as well as other advantages or disadvantages, remains to be explored by comparing CEST-derived kinetic parameters with those extracted using other methods. Here, we present a CEST study for the exchange kinetics between *N*-methyl protons in *N,N*-dimethylacetylamide (DMA), which served as a two-site exchange model with equal populations lacking any resolved *J* coupling. We provided a comparison of different calculation methods, and compared the kinetic data with those from the commonly used technique 2D EXSY.

DMA is one classical example to investigate chemical exchange process of protons between positions with different Larmor frequencies [30,31]. As shown in Fig. 1, the C–N bond between the carbonyl group and the nitrogen atom in this compound has significant double bond character, and limitation of internal rotation around the N–CO bond leads to different chemical environments of the two methyl group connected to the N atom. And thus protons H^a and H^b have accordingly different resonance frequencies, ν_A and ν_B. Intramolecular exchange of the methyl groups contributes to the temperature-dependent phenomenon of the NMR behavior. At room temperature, the exchange rate is small and the residence time of the methyl groups in positions *cis-* or *trans-* in respect to the carbonyl group is relatively long. Consequently, two separate resonances, are observed, with the chemical shifts for H^a and H^b in DMA are 2.95 and 2.79 ppm at 298 K (Fig. 1b), respectively. As the temperature is raised, the signals broaden and finally coalesce to a single one (Fig. S1 in Supporting information) competed with enlarged exchanging rate.

Graphical representation of applied CEST pulse sequence consists of initial continuous saturation pulse, followed by a 90° pulse, shown as in Fig. S2 (Supporting information). In all experiments, CEST attenuation profiles of the methyl protons in DMA were obtained using designated B_1 and T_{sat} values. The rate constants of the methyl protons in DMA were analyzed by fitting observed intensities to the Bloch-McConnell equations (Supporting information) for a system of a single spin exchanging between two states. With the CEST Z-spectrum, a complete CEST profile, a plot of intensity change *vs.* chemical shift of selective saturation was generated to measure the exchange rate between protons H^a and H^b (Fig. 2). Saturation irradiation at H^a or H^b, the transferred protons give a MTR_{asym} of about 57.8%, the value of which is used to quantify CEST effect [32]. To access the exchange rate, a two-site exchange CEST profile was simulated by using Bloch-McConnell equations (QUantifying Exchange using Z-spectrum, QUEZS), whose parameters include ratio of exchange species, longitudinal relaxation rates, transverse relaxation rates and exchange rate constants.

Subsequently, the simulated data were fitted to the experimental data by multi-parameter optimization. The longitudinal relaxation times of H^a and H^b obtained by an inversion recovery experiment were 5.09 and 5.08 s, respectively. The transverse relaxation times were 3.81 and 3.85 s, respectively. The solutions to Bloch-McConnell equations and data fitting procedure are carried out correspondingly. The calculated rate of exchange k_{AB} or k_{BA} is 0.28 s^{-1}. The free energy barrier at 298 K for an exchange process $H^a \leftrightarrow H^b$ from the rate by using Eyring equation [vii] (Supporting information) is +18.2 kcal/mol. Using density function theory at B31YP/6–31g(d) SMD(DMSO) level, internal rotation barrier of N–CO bond in DMA was +18.9 kcal/mol (Fig. S3 in Supporting information). Next, we investigated the exchange rates between protons H^a and H^b at elevated temperatures, and the fitted curves were shown in Figs. 3a and b, indicating that CEST technique combined with Bloch-McConnell equations could be applied to different temperatures in the range of 298∼368 K. The final kinetic curve in Fig. 3c was got according to the *k* data at specified temperatures, and the enthalpy of activation $\Delta H^{\neq}$ and the entropy of activation $\Delta S^{\neq}$ obtained for the exchange process were 14.3 ± 0.6 kcal/mol and −13.0 ± 1.3 cal mol^{-1} K^{-1}, respectively. This method is shown suitable with R^2 of 0.994 for calculating all the exchange rates during the heating process, and further gives kinetic data.

Saturation time T_{sat} and saturation pulse B_1 are two important parameters which influence the CEST effect. Firstly, CEST effect with saturation time T_{sat} of 1, 5, 10, 15, 20 s, and a fixed saturation filed strength B_1 of 5 Hz, was evaluated (Fig. S4 in Supporting information). We found that shorter T_{sat}s could not make the magnetization signal approach the CEST steady state following the spin-lock relaxation rate [33], and then could not offer a good fitting result. In the five experiments studied, the fitting curve at T_{sat} = 1 s deviated obviously from the experimental one. T_{sat} is extended to 5 s or more, especially up to 10, 15 and 20 s, all of R^2 values calculated are approximately equal to 1 (Table S1 in Supporting information). MTR_{asym} of the peak is shown in Fig. 4, to a large extent, removing other effects from the entire Z-spectrum, and it shows that the chemical exchanges between protons H^a and H^b produce remarkable CEST effects, and while an MTR_{asym} of 0.578, corresponding to a 57.8% change in H^a signal approaching the CEST steady state, using a saturation pulse of 5 Hz and a saturation time $T_{sat} \geq 15$ s.

It is noted that the CEST signal strongly depends on the saturation time T_{sat}. The exchange rate between protons H^a and H^b was also estimated by using the Bloch fitting of QUEST data. The CEST contrast for samples was measured with saturation delays of 0.5, 1.0, 1.5, 2.0, 2.5, 3.0, 3.5, 4.0, 4.5, 5.0, 7.0 and 10.0 s, using a saturation power of 5 Hz. The calculated I/I_0 values were then fitted (Fig. 5) using numerical solutions to the Bloch equations, and the

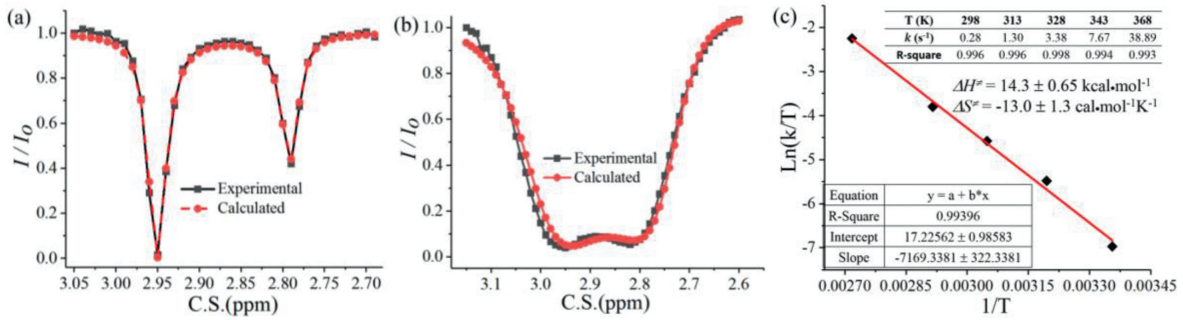

Fig. 3. Calculated and experimental fitted curves of H^a by QUEZS: (a) at 298 K; (b) at 368 K. (c) The kinetic curve according to the *k* data listed.

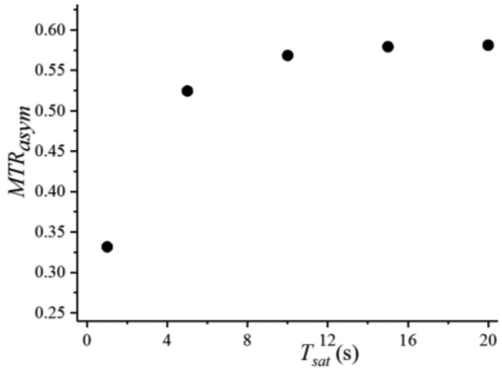

Fig. 4. MTR_{asym} of H^a with varied T_{sat}s at B_1 = 5 Hz, 298 K.

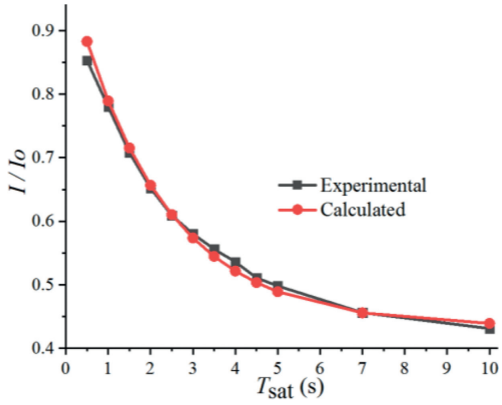

Fig. 5. Calculated and experimental fitted curves of H^a by QUEST at B_1 = 5 Hz, 298 K.

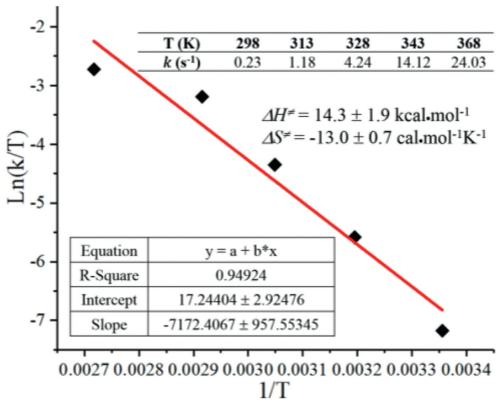

Fig. 6. Chemical exchange rates between protons H^a and H^b by 2D EXSY method at designated temperatures, and T_m = 0.1 s.

k value was estimated to be 0.26, which was in good agreement with the above results.

Secondly, CEST signals with saturation pulse B_1 of 1, 5, 10, 15, 20 Hz, and a fixed saturation time T_{sat} of 15 s, were also investigated, and all give reliable results (Fig. S5 and Table S2 in Supporting information). This indicates that although the amplitude of B_1 affects the band width of the Z-spectrum, it hardly affects the fitting results when T_{sat} is long enough. Meanwhile, we also tried to investigate the effect of B_1 on the exchange rate, at a short T_{sat}. Surprisingly at a fixed short T_{sat} = 1 s, varied B_1s in a small range could not provide obvious attenuation. This is quite different from the experiment of CEST in MRI. There is no large adjustable range of B_1, due to the small spectral width of the studied nucleus. Therefore, it is not advisable to exploit the QUantifying Exchange using Saturation Power (QUESP) method to calculate the exchange rate in this system.

The two-dimensional exchange spectroscopy, 2D EXSY technique, was also used to measure the exchange process between protons H^a and H^b in DMA. This gives us the opportunity to compare both 1D CEST and 2D EXSY data for exchange rate measurements at various temperatures. Based on 2D EXSY spectrum, the exchange rates between H^a and H^b were obtained, and the *k* values at designated temperatures were listed in Fig. 6. With 2D EXSY, the intercept and slope of the fitted curve are almost the same as the values in Fig. 3c, however, its R^2 is 0.949. The five *k* points obtained by 2D EXSY deviated obviously regardless of whether it is at low or high temperatures, especially compared to those of CEST. The accurate *k* measurement by 2D EXSY strongly depends upon the T_m and the relaxation delay Tdelay, and thus poor temperature compliance with fixed parameters, and in addition, it also depends on concentration of the investigated system [34]. And thus, the CEST technique is simpler, and could not only obtain the kinetic data comparable to 2D EXSY, but also its R^2 is more close to 1. Furthermore, the only requirements for CEST are the existence of a chemical exchange in the slow exchange regime on the NMR time scale ($k \leq |\Delta\nu|$) and one of the chemical exchange species being visible in conventional NMR experiments [35]. It could detect invisible species, which could not be accomplished by 2D EXSY or other NMR techniques.

CEST technique, which is very suitable for slow exchange systems, has attracted immense interest, owing to its simple, the high sensitivity and non-invasive. In recent years, its application has been gradually expanded to various fields, especially in tracking the slow chemical process, as long as it meets the only requirement of $k \leq |\Delta\nu|$ on the NMR time scale. In this study, we chose DMA as a classic example, and presented clearly how this new tool could study the kinetics of a slow chemical exchange between two sites. We provided a comparison of different calculation methods,

including QUEZS and QUEST, and studied the influence of two important parameters T_{sat} and B_1 on the Bloch-McConnell equations. And, QUESP used in MRI commonly was also confirmed not applicable in this investigated system. CEST technique is more suitable for calculating all the exchange rates at a wide range of temperatures, and further gives accurate kinetic data, especially compared to 2D EXSY. It is believed that CEST NMR method will provide new ideas for organic chemists and chemical biologists, and unveil of dynamic kinetics for more systems.

Declaration of competing interest

The authors declare that they have no known competing financial interests or personal relationships that could have appeared to influence the work reported in this paper.

Acknowledgments

This research was supported under the National Natural Science Foundation of China (Nos. 22077123 and 21977099). We thank Prof. M. T. McMahon for the simulation code, and Mr. Tengyu Huang from ICCAS for the simulation of Bloch-McConnell equations and Mr. Hao Zhou from ICCAS for the calculation of the internal rotation barrier of DMA.

Supplementary materials

Supplementary material associated with this article can be found, in the online version, at doi:10.1016/j.cclet.2022.01.022.

References

[1] M. Chiarucci, A. Ciogli, M. Mancinelli, S. Ranieri, Angew. Chem. Int. Ed. 53 (2014) 5405–5409.
[2] M. Yamada, H. Narita, Y. Maeda, Angew. Chem. Int. Ed. 59 (2020) 16133–16140.
[3] K.K. Mishra, S.K. Singh, S. Kumar, et al., J. Phys. Chem. A 123 (2019) 5995–6002.
[4] M. Novakovic, M.D. Battistel, H.F. Azurmendi, et al., J. Am. Chem. Soc. 143 (2021) 8935–8948.
[5] L.X. Wang, B.Q. Hu, J.F. Xiang, et al., Tetrahedron 70 (2014) 8588–8591.
[6] L. Nisius, S. Grzesiek, S. Key, Nat. Chem. 4 (2012) 711–717.
[7] J.W. Li, Y.F. Wang, L.Y. An, J.F. Chen, L.S. Yao, J. Am. Chem. Soc. 140 (2018) 3194–3197.
[8] P. Kukic, D. Farrell, L.P. McIntosh, et al., J. Am. Chem. Soc. 135 (2013) 16968–16976.
[9] L.Y. An, Y.F. Wang, N. Zhang, et al., J. Am. Chem. Soc. 136 (2014) 12816–12819.
[10] E. Demetriou, A. Kujawa, X. Golay, Prog. Nucl. Magn. Reson. Spectrosc. 120-121 (2020) 25–71.
[11] L.M. Jackman, F.A. Cotton, Dynamic Nuclear Magnetic Resonance Spectroscopy, Academic Press, New York, San Francisco, London, 1975.
[12] S. Forsen, R.A. Hoffman, J. Chem. Phys. 39 (1963) 2892–2901.
[13] G. Liu, Y. Liang, A. Bar-Shir, et al., J. Am. Chem. Soc. 133 (2011) 16326–16329.
[14] J. Zhou, J.F. Payen, D.A. Wilson, R.J. Traystman, P.C. van Zijl, Nat. Med. 9 (2003) 1085–1090.
[15] P.C. van Zijl, N.N. Yadav, Magn. Reson. Med. 65 (2011) 927–948.
[16] D. Ryoo, X. Xu, Y.G. Li, et al., Anal. Chem. 89 (2017) 7758–7764.
[17] C.O. Miller, J. Cao, E.Y. Chekmenev, et al., Anal. Chem. 87 (2015) 5824–5830.
[18] N. Lokesh, A. Seegerer, J. Hioe, R.M. Gschwind, J. Am. Chem. Soc. 140 (2018) 1855–1862.
[19] V. Ramanujam, C. Charlier, A. Bax, Angew. Chem. Int. Ed. 58 (2019) 15309–15312.
[20] M.S. Jeletic, C.E. Lower, I. Ghiviriga, A.S. Veige, Organometallics 30 (2011) 6034–6043.
[21] B. Zhao, S.L. Guffy, B. Williams, Q. Zhang, Nat. Chem. Bio. 13 (2017) 968–974.
[22] B. Zhao, J.T. Baisden, Q. Zhang, J. Mag. Reson. 310 (2020) 106642–106648.
[23] A. Rangadurai, H.L. Shi, H.M. Al-Hashimi, Angew. Chem. Int. Ed. 59 (2020) 1–6.
[24] H. MalcomLevitt, in: Spin Dynamics: Basics of Nuclear Magnetic Resonance, 2nd ed., John Wiley & Sons, Chichester, UK, 2001, p. 686.
[25] V. Guivel-Scharen, T. Sinnwell, S.D. Wolff, R.S. Balaban, J. Magn. Reson. 133 (1998) 36–45.
[26] K. Ward, A. Aletras, R.S. Balaban, J. Magn. Reson. 143 (2000) 79–87.
[27] M.T. McMahon, A.A. Gilad, J. Zhou, et al., Magn. Reson. Med. 55 (2006) 836–847.
[28] D.E. Woessner, S. Zhang, M.E. Merritt, A.D. Sherry, Magn. Reson. Med. 53 (2005) 790–799.
[29] M. Zaiss, P. Bachert, Phys. Med. Biol. 58 (2013) R221–R269.
[30] J. Jeener, B.H. Meier, P. Bachmann, R.R. Ernst, J. Chem. Phys. 71 (1979) 4546–4553.
[31] O.W. Sørensen, G.W. Eich, M.H. Levitt, G. Bodenhausen, R.R. Ernst, Prog. Nucl. Magn. Reson. Spectrosc. 16 (1983) 163–192.
[32] T. Jin, S. Kim, Magn. Reson. Med. 82 (2019) 1876–1889.
[33] P.Z. Sun, Magn. Reson. Med. 85 (2021) 3281–3289.
[34] K. Nikitin, R. O'Gara, Chem. Eur. J. 25 (2019) 4551–4589.
[35] G. Liu, X. Song, K.W. Chan, M.T. McMahon, NMR Biomed. 26 (2013) 810–828.